Article

A Soil Moisture and Vegetation-Based Susceptibility Mapping Approach to Wildfire Events in Greece

Kyriakos Chaleplis [1,*], Avery Walters [2], Bin Fang [2], Venkataraman Lakshmi [2] and Alexandra Gemitzi [1,2]

1   Department of Environmental Engineering, Democritus University of Thrace, V. Sofias 12, 67100 Xanthi, Greece; agkemitz@env.duth.gr
2   Department of Civil and Environmental Engineering, University of Virginia, 151 Engineers Way, Charlottesville, WV 22904, USA; acw4mhp@virginia.edu (A.W.); bf3fh@virginia.edu (B.F.); vlakshmi@virginia.edu (V.L.)
*   Correspondence: kchalepl@env.duth.gr

Abstract: Wildfires in Mediterranean areas are becoming more frequent, and the fire season is extending toward the spring and autumn months. These alarming findings indicate an urgent need to develop fire susceptibility methods capable of identifying areas vulnerable to wildfires. The present work aims to uncover possible soil moisture and vegetation condition precursory signals of the largest and most devastating wildfires in Greece that occurred in 2021, 2022, and 2023. Therefore, the time series of two remotely sensed datasets–MAP L4 Soil Moisture (SM) and Landsat 8 NDVI, which represent vegetation and soil moisture conditions—were examined before five destructive wildfires in Greece during the study period. The results of the analysis highlighted specific properties indicative of fire-susceptible areas. NDVI in all fire-affected areas ranged from 0.13 to 0.35, while mean monthly soil moisture showed negative anomalies in the spring periods preceding fires. Accordingly, fire susceptibility maps were developed, verifying the usefulness of remotely sensed information related to soil moisture and NDVI. This information should be used to enhance fire models and identify areas at risk of wildfires in the near future.

Keywords: SMAP soil moisture; Landsat 8 NDVI; fire susceptibility mapping; fire precursory signals; vulnerability to disasters

1. Introduction

Wildfires are increasingly impacting the natural environment and human lives. They are exhibiting increased frequency and greater destruction, posing significant societal challenges [1,2]. The impact of climate change on wildfire occurrence has been studied in many previous works, and researchers have reached a consensus on exceptionally high global fire activity, with increased burned area and fire frequency [3,4]. Also, a high spatial variability of fire changes has been observed. Some areas show little or no change or even a decrease in fire occurrences [1]. The need to study the underlying mechanisms of various ecological variables involved in wildfires has been identified in previous research, with the ultimate goal of understanding the expected causes and consequences of future wildfires and adjusting fire management strategies [1,2,5]. Wildfires also affect the carbon cycle as they are found to account for almost 35% of global carbon emissions, impacting global greenhouse gas emissions [6]. They also affect carbon sequestration during the regeneration processes of burned forests, as increased vegetation productivity is observed in fire-affected areas after the wildfire events [7].

Previous research has shown that many variables are involved in the outbreak of wildfires, with weather, fuel, and human activities playing synergistic roles [8]. Thus, in Mediterranean areas, a prolonged fire season has been found, and changes in fire frequency and burned areas have been reported [9]. Meteorological conditions have also been reported to impact extreme fire risk in the Mediterranean, and the Fire Weather Index

(FWI) was used in previous works to quantify fire danger [10,11]. In Australia, wildfire activity was found to be impacted by changes in climate variables during the three-month period preceding the fire season [12]. The warming climate is expected to increase the vulnerability of ecosystems to wildfires [13]. Indices that quantify fuel properties, such as fuel accumulation and moisture, are also known to play an important role in wildfire occurrence [13,14]. Poor forest management has also been identified as a factor contributing to increased fire occurrence due to the limited budget required for the adoption of fire prevention measures [15,16].

Determination of areas at high risk of wildfire occurrence is essential to guide forest management practices and protect ecosystem services. Indices related to vegetation greenness, such as the Normalized Difference Vegetation Index (NDVI) and Enhanced Vegetation Index (EVI), along with other environmental variables like elevation, slope, precipitation, and temperature, have been extensively analyzed, and their contributing role in wildfire occurrence has been clarified in many regions around the world [17–23]. Soil moisture has also been known to play a key role in wildfire occurrence due to the control of vegetation growth [8,13,24], but the lack of available information at the global scale restricted relevant research to case studies at the local scale [8]. Recent advances in satellite-based soil moisture retrievals have enabled scientists to evaluate potential links of soil moisture with wildfires at larger scales [8,13,24,25]. In this manner, previous works demonstrated the relationship between earlier snowmelt and associated decreased soil moisture in summer and wildfire occurrence in Western U.S. [26]. The potential of remotely sensed C-band Sentinel-1A data to accurately describe the forest fuel moisture content was indicated in previous studies [27]. Moreover, Soil Moisture Active Passive (SMAP) mission soil moisture retrievals are found to be quite useful in the estimation of Live Fuel Moisture in chaparral areas [28], indicating their usefulness in acquiring information on vegetation dryness and fire risk. A global study incorporating a large number of wildfire events indicated that although fire events are quite complex phenomena and the individual contribution of specific environmental parameters is challenging, satellite soil moisture can offer improved fire forecasting in the estimation of the possibility of ignition and the size of affected [8] and improve fire forecasting at the global scale [29]. Analogous findings were reported in Australia and California, where SMAP soil moisture proved to be a reliable predictor for large wildfires and suitable for wildfire susceptibility [30]. Another study in nine patches of tallgrass prairie under patch-burn management in Oklahoma, USA, indicated that the results of grassland fuelbed models could be improved by incorporating soil moisture observations [31]. Furthermore, fire forecasting applications for agriculture have successfully implemented SMAP SM into a global operational crop forecasting system, especially for monitoring drought conditions in agricultural areas, supporting decision-making for global food security [32].

The motivation of the present work was the increase in fire-affected areas, fire severity and destructiveness, the lengthening of fire occurrence season, and the diversity of forest types affected during the last few years, i.e., from 2021 onwards, and their possible relation to the persistent drought that Greece experienced during this period. Thus, the time series of the two variables that are indicative of the vegetation and soil moisture conditions were examined for the five most destructive wildfires in Greece during the study period. The time series of SMAP Level-4 (L4) SM and the Landsat 8 NDVI were retrieved and evaluated in the fire-affected areas. Initially, SMAP L4 SM data were compared against in situ soil moisture measurements from a monitoring network in NE Greece, and results indicated that SMAP L4 SM is representative of the moisture conditions and that the time series of SM and NDVI demonstrate specific properties in the fire-affected areas, which can be useful for fire susceptibility mapping. Furthermore, to highlight the social aspect, the results of the fire susceptibility mapping in this work were analyzed in conjunction with vulnerability to disasters in Europe, estimated by the EU Disaster Risk Management Knowledge Center (DRMKC) [33,34].

2. Methods

2.1. Description of the Study Area and the Wildfire Events

In the present work, the data related to the 11 most important wildfire events in terms of area (area affected > 25 km^2) and destructiveness in Greece from 2021 to 2023 were collected from the Hellenic Fire Service database [35]. Details on the delineation methodology of the fire-affected areas and the specific fire impacts on various economic sectors can be found in Supplementary Material (Table S1). The specific time frame was selected because of the sharp increase in fire activity that was observed during that period, according to data provided by the European Forest Fire Information System (EFFIS) [36]. The first five wildfires in Table 1 were used to develop the methodology, while the other six were used in the verification of the approach. Additionally, smaller fire events detected in the MODIS Fire Information for Resource Management System (FIRMS) [37] dataset on active fires were also incorporated in the validation of the developed approach.

Table 1. List of the wildfires and their properties analyzed in the present work.

No.	Location	Dates	Area (km^2)	Land Cover	Cause
1	Evia island (North Evia)	3 August 2021	511.8	Arable land, permanent crops, heterogeneous agricultural areas, forests; shrub and/or herbaceous vegetation association, and open spaces with little or no vegetation	Combination of human activities, increased fuel accumulation, and meteorological conditions (burning of agricultural residues)
2	Alexadroupolis-Dadia (Evros)	19 August 2023	1000.2	Forests, shrub and/or herbaceous vegetation association, heterogeneous agricultural areas, arable land, permanent crops, and pastures	Possible thunder activity. A wildfire started on the 19th of August early in the morning in a forest area near Aristino village (East Macedonia and Thrace Region).
3	Sostis and Gratini villages at Rhodope	21 August 2023	28.3	Mixed forests, arable land, shrub and/or herbaceous vegetation association, heterogeneous agricultural areas, pastures, and open spaces with little or no vegetation	Combination of human activities, increased fuel accumulation, and meteorological conditions
4	Rhodes Island (Central and SE)	1 Julie 2023	178.0	Shrub and/or herbaceous vegetation association, heterogeneous agricultural areas, forests, permanent crops, arable land, open spaces with little or no vegetation, and pastures	Combination of human activities (old dump), increased fuel accumulation, and meteorological conditions
5	Lesvos island (Vattera)	23 Julie 2022	25.5	Arable land, permanent crops, heterogeneous agricultural areas, forests, shrub and/or herbaceous vegetation association, and other	Human activities (burning of agricultural residues)
6	Papikio Mt at Rhodope	22 October 2022	25.6	Complex cultivation patterns; land principally occupied by agriculture, with significant areas of natural vegetation; broad-leaved and mixed forest; natural grassland; sclerophyllous vegetation; transitional woodland shrub; and sparsely vegetated areas	Combination of human activities, increased fuel accumulation, and meteorological conditions
7	Varibobi (Attica)	03 August 2021	83.8	Arable land, permanent crops, pastures, heterogeneous agricultural areas, forests, shrub and/or herbaceous vegetation association, and open spaces with little or no vegetation	Electricity network. From Tuesday 03 August 2021 afternoon, wildfires were raging in the northeast sector of the Attica region in Greece.

Table 1. *Cont.*

No.	Location	Dates	Area (km²)	Land Cover	Cause
8	Diavolitsi (Messinia Peloponnese)	04 August 2021	51.1	Non-irrigated arable land; olive groves; pastures; complex cultivation patterns; land principally occupied by agriculture; with significant areas of natural vegetation; broad-leaved forest; coniferous forest; mixed forests; natural grassland; sclerophyllous vegetation; beaches, dunes, and sand plains; and sparsely vegetated areas	Combination of human activities, increased fuel accumulation, and meteorological conditions
9	Gerania Mt (Corinthia)	19 May 2021	69.6	Arable land, permanent crops, heterogeneous agricultural areas, forests, shrub and/or herbaceous vegetation association, and open spaces with little or no vegetation	Human activities (burning of agricultural residues); A large wildfire burning large areas of pine forest in the area of Schinos, in Corinthia prefecture.
10	Penteli (Attica)	19 Julie 2022	27.9	Shrub and/or herbaceous vegetation association, forests, heterogeneous agricultural areas, and coniferous forest	Combination of human activities, increased fuel accumulation, and meteorological conditions. A forest fire broke out on the slopes of Mount Penteli in the northern suburbs of Athens.
11	Parnitha (Attica)	22 August 2023	61.9	Forest, pastures, heterogeneous agricultural areas, open spaces with little or no vegetation, and shrub and/or herbaceous vegetation association. A total of 47% of the area is protected.	The fire is attributed to a combination of human activities and meteorological conditions.

Regarding the causes of most wildfire events, they are generally attributed to heat waves, which become more frequent due to climate change in combination with the accumulation of dry vegetation, mainly due to poor forest management, as well as to human activities—either arson or negligence—and also to lightning activity [14]. The varied nature of land cover types, timing, and prevailing weather conditions make evaluating the fire-triggering mechanisms of specific events quite challenging as case studies. For example, both wildfires in the Rhodope area in NE Greece (No. 3 and 6 in Table 1) occurred in mixed forest areas in a mountain area that had never been impacted in the past by such large fires. Notably, event No. 6 in Table 1 started in late October 2022 and lasted until the 20th of November 2022, a period that is outside the fire season, especially for North Greece. The tables in Supplementary Material Table S1 detail the consequences of each of the eleven fires. The spatial distribution of wildfires can be seen in Figure 1. From this, it seems that fire activity is becoming more diverse and affects areas that were not previously considered susceptible to fire.

2.2. Description of Data and Analysis

In this work, we built upon previous studies that have identified SM and NDVI as suitable variables to capture the spatial and temporal changes in vegetation conditions [13,14,17,18]. We also focused on a remotely sensed-only approach to exploit the advantages of remote sensing regarding its spatial coverage and temporal repeat for global environmental monitoring. To evaluate the possible precursory signal of soil moisture for fire occurrence, we evaluated remotely sensed SM from SMAP and, more specifically, the SMAP L4 dataset [38]. Additionally, the USGS Landsat 8 Level 2, Collection 2, Tier 1 product, at 30 m spatial resolution, was used to evaluate monthly NDVI values for the study period as a proxy for vegetation conditions. Both the SM and NDVI time series were evaluated for approximately a 2-year period prior to fire occurrence.
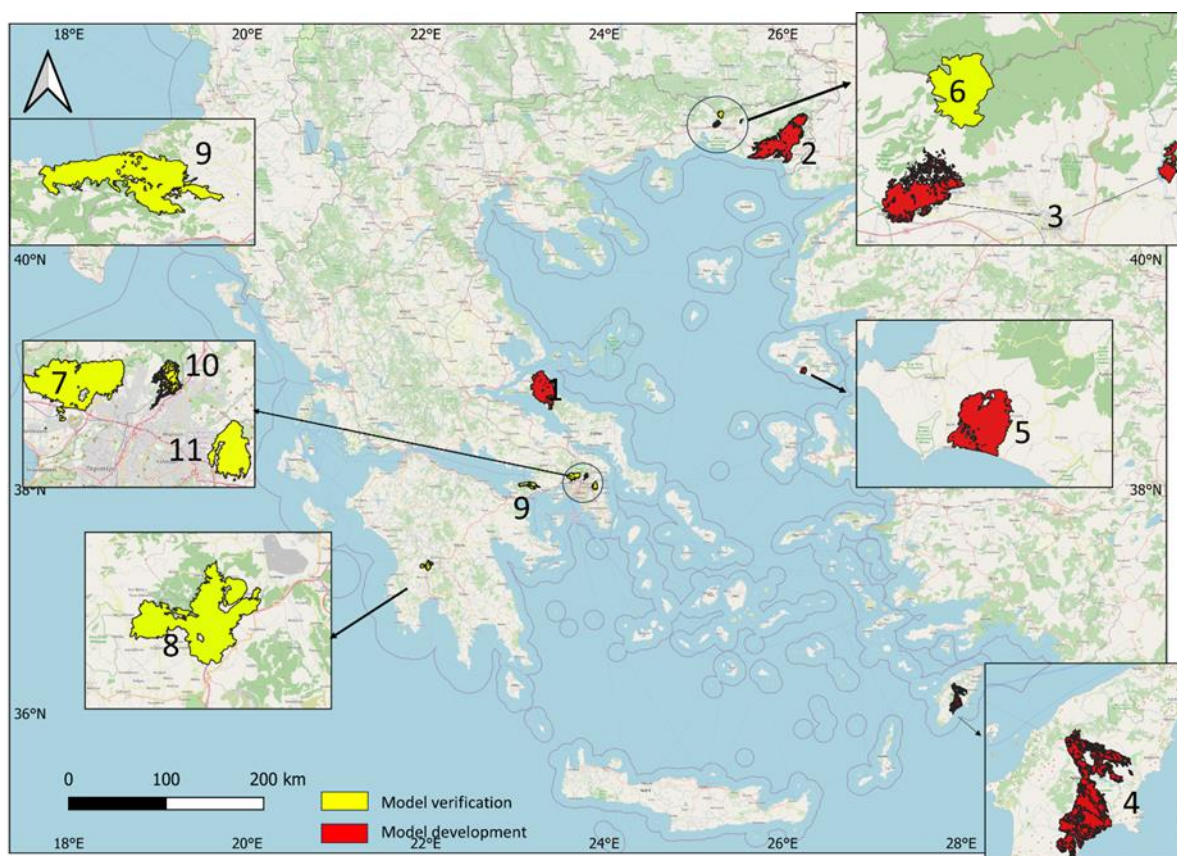
Figure 1. Location map of the wildfires analyzed in the present work. Numbers correspond to those indicated in Table 1. Red designated areas correspond to wildfires that are used for the method development (Fires 1–5), while yellow is used for verification (Fires 6–11) only.

Since remotely sensed SM at a reasonable spatial resolution for such analysis has only recently been made available, i.e., from 2015 until the present, and not much research is available on its relationship to wildfire occurrence, we also evaluated the correlation of the annual averages of SMAP L4 SM over Greece, with the number of fires and size of impacted areas. Additionally, to verify that SMAP L4 SM provides consistent SM observations in the study area, a comparison of SMAP L4 surface SM and root zone SM was conducted with data from three in situ sensors operated by Democritus University of Thrace in NE Greece, with Sentek Drill and Drop single-point soil moisture and soil temperature sensors (https://sentektechnologies.com/products/soil-data-probes/drill-drop/, accessed on 1 March 2024), measuring at a depth of 5–10 cm, from 2021 until today. The in situ sensors were calibrated prior to their installation using oven drying at 110 °C for 24 h of soil samples, according to the methodology described by the Australian Department of Sustainable Natural Resources and the Australian National Soil Strategy [39]. The area where SM sensors operate is Papikio Mt., an area affected twice by wildfires in 2022 and 2023 (events No. 3 and 6 in Table 1). Daily SM values were averaged at the monthly time step and compared to SMAP acquisitions.

The SMAP L4 soil moisture product [38,40,41] includes surface soil moisture (0–5 cm vertical average), root-zone soil moisture (0–100 cm vertical average), and additional modeled parameters like soil temperature, evapotranspiration, and net radiation, along with meteorological forcing variables. L-band brightness temperature from the SMAP half-orbit passes at around 6:00 a.m. and 6:00 p.m. local solar time and is assimilated into a land surface model. SMAP L4 thus provides global 3-hourly time-averaged geophysical data fields from the assimilation system at 9 km spatial resolution from March 2015 to the present. Wildfire perimeter polygons were taken from the Hellenic Fire Service database [35] and

then used in the Google Earth Engine platform [42]. The SMAP L4 Global 3-hourly 9 km Surface and Root Zone Soil Moisture was then retrieved and processed by implementing a JavaScript code (available in the code availability section of the present work) in order to estimate average monthly SM values in the affected areas. Monthly anomalies were then computed as the difference of the asset month relative to the same month averaged across the time series (from 2015 to the present), excluding the asset year. In a similar way, Landsat 8 NDVI was extracted for the fire polygons, and time series graphs were prepared. Based on the properties of SM and NDVI time series prior to fire events, a fire susceptibility mapping approach was proposed.

To evaluate the social impact, the Vulnerability to Disasters Indicator (VDI) estimated by the EU DRMKC was examined along with the fire susceptibility mapping of our work. The VDI is a cross-scale EU-wide indicator that supports the evaluation of disaster risk from multiple hazards [33,34]. It encompasses five dimensions—the social, economic, political, environmental, and physical—across three different administrative levels (i.e., Country scale, NUTS2, and NUTS3). Scores of the VDI range from 0 to 10. The dataset corresponding to Greek territory at the NUTS3 level for 2021, 2022, and 2023 was accessed from the DRMKC Risk Data Hub (RDH) (https://drmkc.jrc.ec.europa.eu/risk-data-hub/#/dashboardvulnerability, accessed on 10 March 2024). The 2023 VDI data set corresponds to VDI forecasts by DRMKC, as the actual 2023 VDI estimates were not available by the time of completion of the present work. The whole process is described in the flow chart of Figure 2.
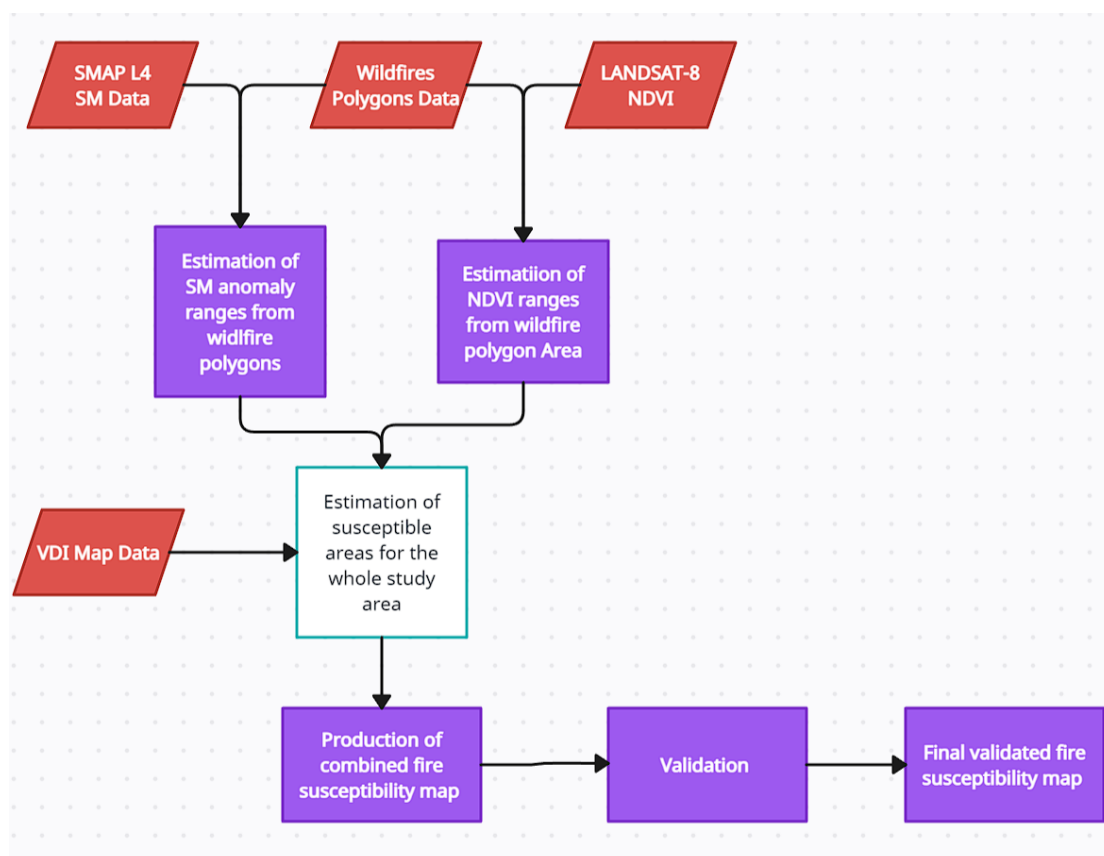

Figure 2. Fire susceptibility map flow chart.

3. Results

Figure 3 demonstrates the time series graphs of country-averaged monthly SMAP L4 SM with the number of fires (Figure 3a) and the size of affected areas (Figure 3b) during the fire season, i.e., June to August. The correlation coefficient (r) for SM and the number of fires was found to be −0.57, while the correlation coefficient for SM and the size of

the affected areas was −0.62. Both were found significant at $p < 0.001$. Details on the significance tests can be found in Tables S2 and S3 in Supplementary Material. Additionally, we tested for significance after removing linear trends from the examined time series, and it was found that significance still holds at $p < 0.002$ for the detrended time series (Results on the significance testing of the detrended time series can be found in Tables S4 and S5 in Supplementary Material)).
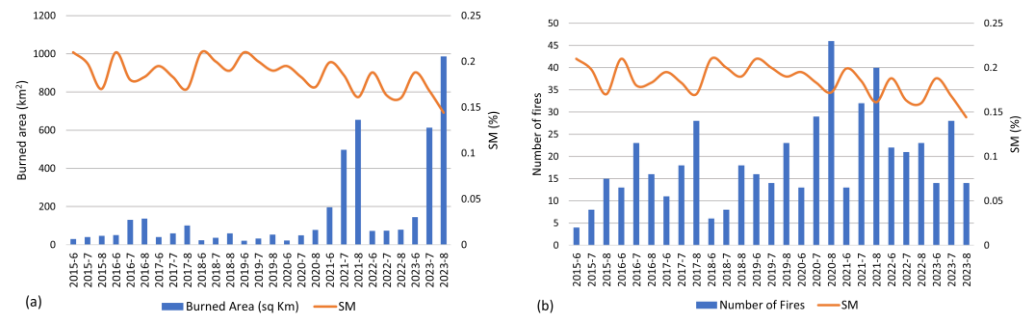

Figure 3. Time series of soil moisture and (**a**) number of fires, (**b**) burned area, in Greece (2015–2023).

Both negative coefficients indicate inverse correlation, i.e., decreasing values of SM correspond to increased number of fires and size of affected areas. Moreover, although the number of fires after 2020 demonstrated a decreasing trend, the size of areas affected showed a sharp increase from 2021 forward, indicating the enhanced destructiveness of wildfires. The Alexandroupolis-Dadia mega-fire event in August 2023 is a characteristic case, being one of the largest wildfires in the history of Europe. Analogous changes in fire impacts were reported in Spain [4], where since 2014, a smaller number of fires proved to be capable of destroying larger land areas.

A comparison of the monthly average SMAP L4 root zone SM and surface SM with the averages of the three monitoring points in Rhodope area (NE Greece) can be found in Figure 4. Averaging over the three monitoring points was necessary due to the different footprints of SMAP L4, i.e., 9 km and the point values of in situ SM sensors.
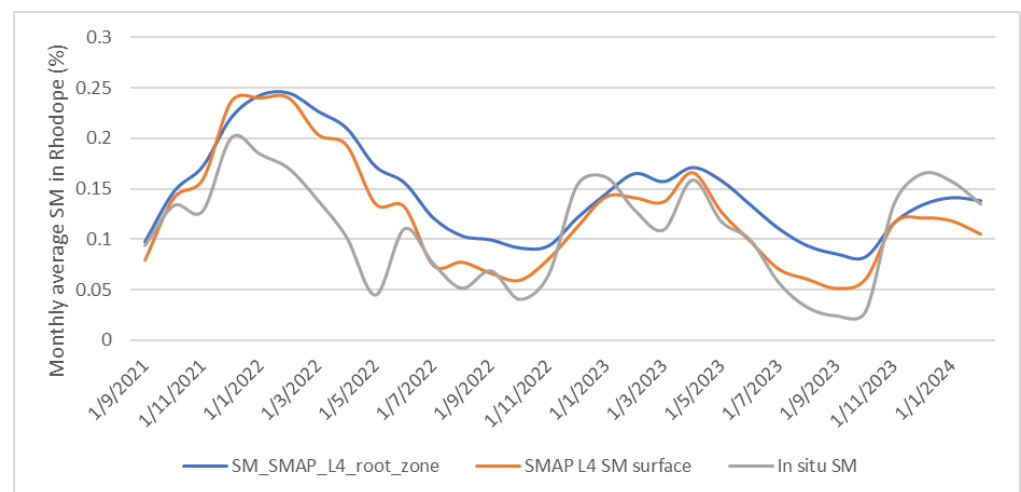

Figure 4. Comparison of in situ SM data and SMAP L4 surface SM and root zone SM in the Rhodope area (NE Greece) during the study period.

Analysis of the data in Figure 4 indicated r values of 0.70 for in situ SM and root zone SMAP SM and r = 0.78 for surface SMAP SM (significant at the $p < 0.001$ level). To verify that significance still holds after removing linear trends from the examined time series, correlation tests were performed at the detrended time series, and the results are significant at the $p < 0.001$ level also for the detrended time series (Tables S6 and S7 in Supplementary Material). Although the comparison corresponds to only a small portion of the country

area, and the two data sets are quite different in terms of footprint and acquisition approach, it can still be regarded as an indication of the consistency between ground measurements and SMAP L4 acquisitions. Moreover, SMAP SM has been extensively validated in many other areas around the world and is considered a reliable dataset for a wide range of environmental applications [30,32,43,44]. Surface SMAP SM is better correlated to the in situ dataset compared with root zone SMAP SM. This is perhaps due to the description of the entire root zone, i.e., 0–100 cm of the SMAP L4 root zone SM, and not of the top layer, which is represented by the in situ measurements and is closer to the SMAP L4 surface SM. Thus, SMAP L4 surface SM was used for the analysis in the present work.

The results of temporal analysis are presented in Figure 5. Regarding NDVI, no specific temporal trends were observed in the studied fire-affected areas, except for the expected seasonal fluctuations in the pre-fire occurrence period. However, the mean NDVI in the periods prior the fire events ranged from 0.13 to 0.35, indicating low moisture vegetation conditions.

On the contrary, SMAP L4 surface SM demonstrated a distinctive decreasing trend for at least one year before fire events. A specific pattern observed in average SM is the occurrence of negative mean SM anomaly, dropping lower than −5%, during the preceding springs. Even in the case of Rhodes Island, where May 2023 was a relatively wet month, the mean SM anomaly during spring remained within negative values lower than −5%. In Figure 6, it is evident that all fire-affected areas are within this negative SM anomaly zone, with the most indicative cases being the Alexandroupolis-Dadia and Rhodes wildfires (both in 2023). These indicate how decreased moisture conditions designate areas of increased fire occurrence risk. Thus, in the present work, based on the above findings, we proposed a spatial susceptibility mapping approach based on the presence of negative mean SMAP L4 surface SM anomalies in the spring prior to fire occurrence, lower than −5% and within the specified range of Landsat 8 derived NDVI values, i.e., 0.13–0.35. Thus, the selection criteria become mean spring SM anomaly <−5% and 0.13 < NDVI < 0.35). At the country level, this SM anomaly corresponds to approximately mean minus two standard deviations of SM, although for each specific fire-affected area, this threshold might correspond to a slightly different standard deviation threshold, indicating thus that the examined areas experience extreme drought conditions.
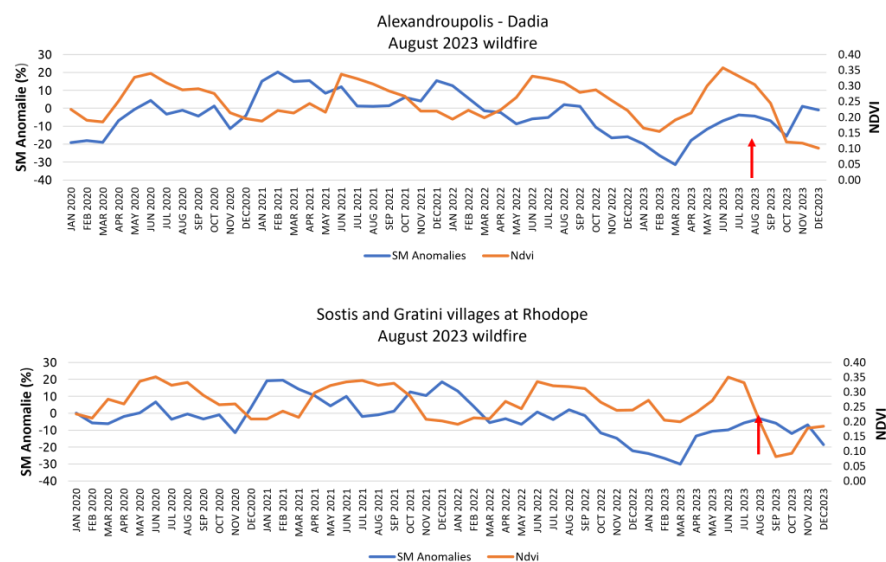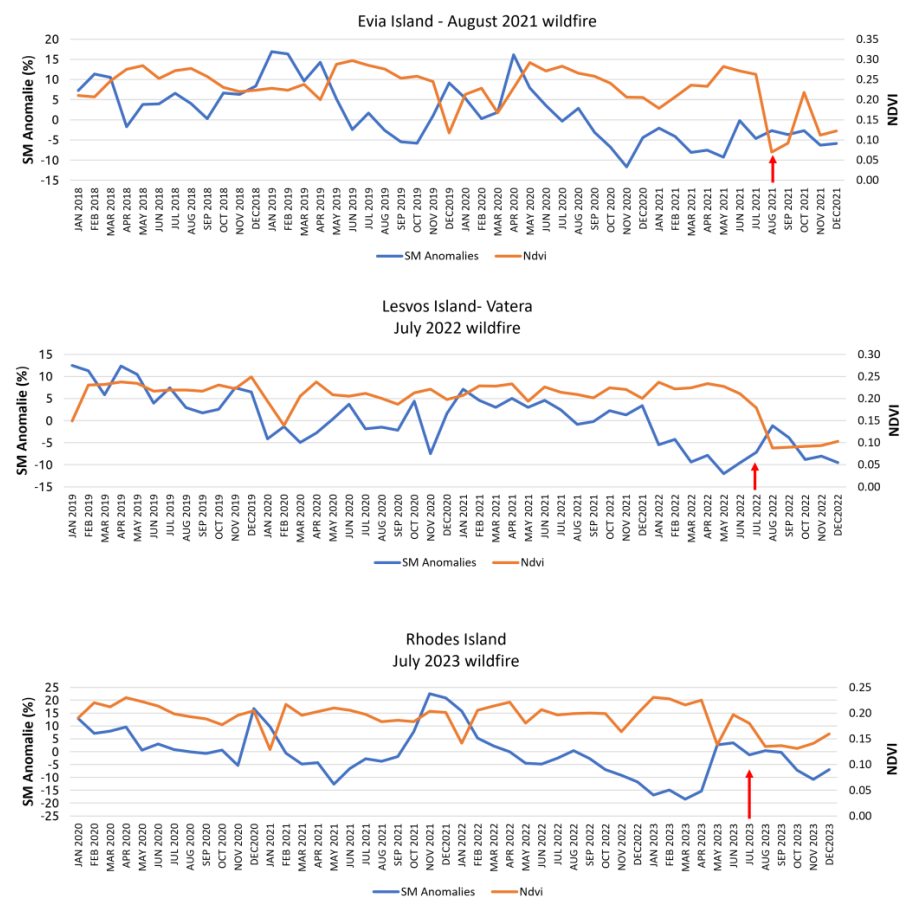

Figure 5. *Cont.*

Figure 5. Time series graphs of NDVI and SMAP L4 surface SM anomalies for five wildfires during 2021–2023 in Greece. Arrows indicate the date of wildfire occurrence.
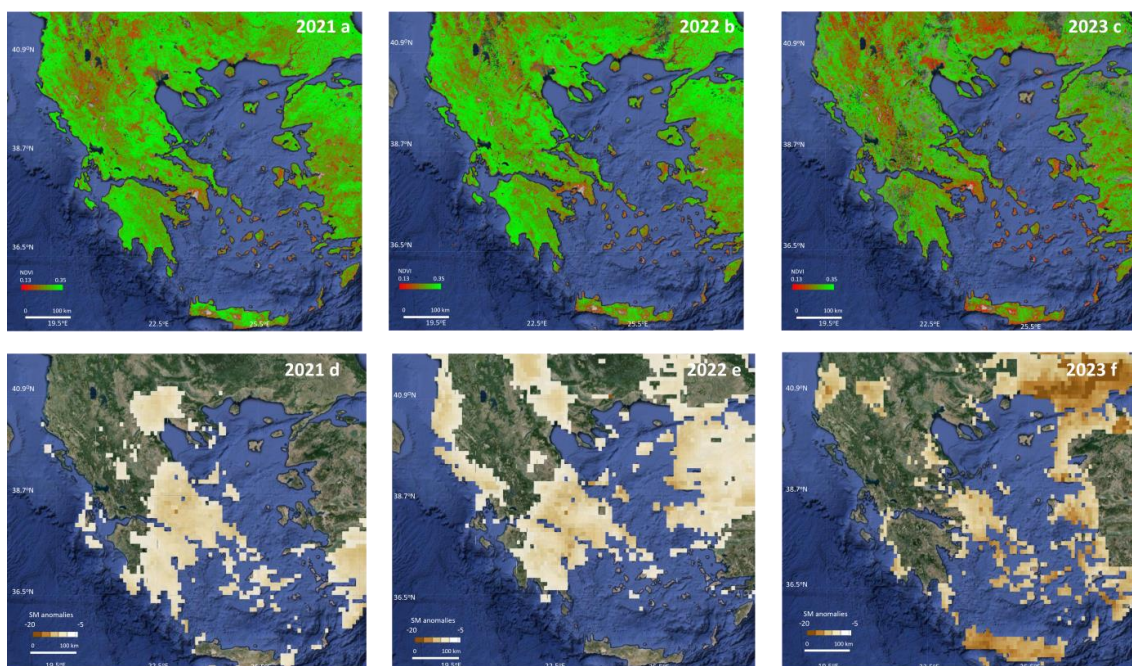

Figure 6. Spatial distribution of NDVI (**a**–**c**) and SM anomalies (**d**–**f**) satisfying the fire susceptibility criteria in the broader area of Greece for 2021, 2022, and 2023.

Figure 6 presents the spatial distribution of areas demonstrating negative mean SMAP L4 SM anomalies of -5% during spring 2021, 2022, and 2023, respectively (Figure 6d–f), and the spatial distribution of areas within the NDVI range of 0.13–0.35 for the same periods (Figure 6a–c). The final susceptibility maps for each examined year are produced by selecting pixels that reach both those predefined criteria regarding SM, i.e., negative mean SM anomalies < -5%, and NDVI in the range of 0.13–0.35 for the preceding spring. The results can be found in Figure 7. To verify the results, fire events 6 to 11 (Table 1) were overlaid with the fire susceptibility maps (Figure 7a–c). All events fall within the fire-susceptible areas, as defined by the present methodology. Also, the vast majority of FIRMS-detected fires are found within the fire-susceptible locations. In Table 2, the results of the fire susceptibility mapping methodology are presented, where it can be seen that the success rate of the susceptibility mapping ranges from 83% to 87%.
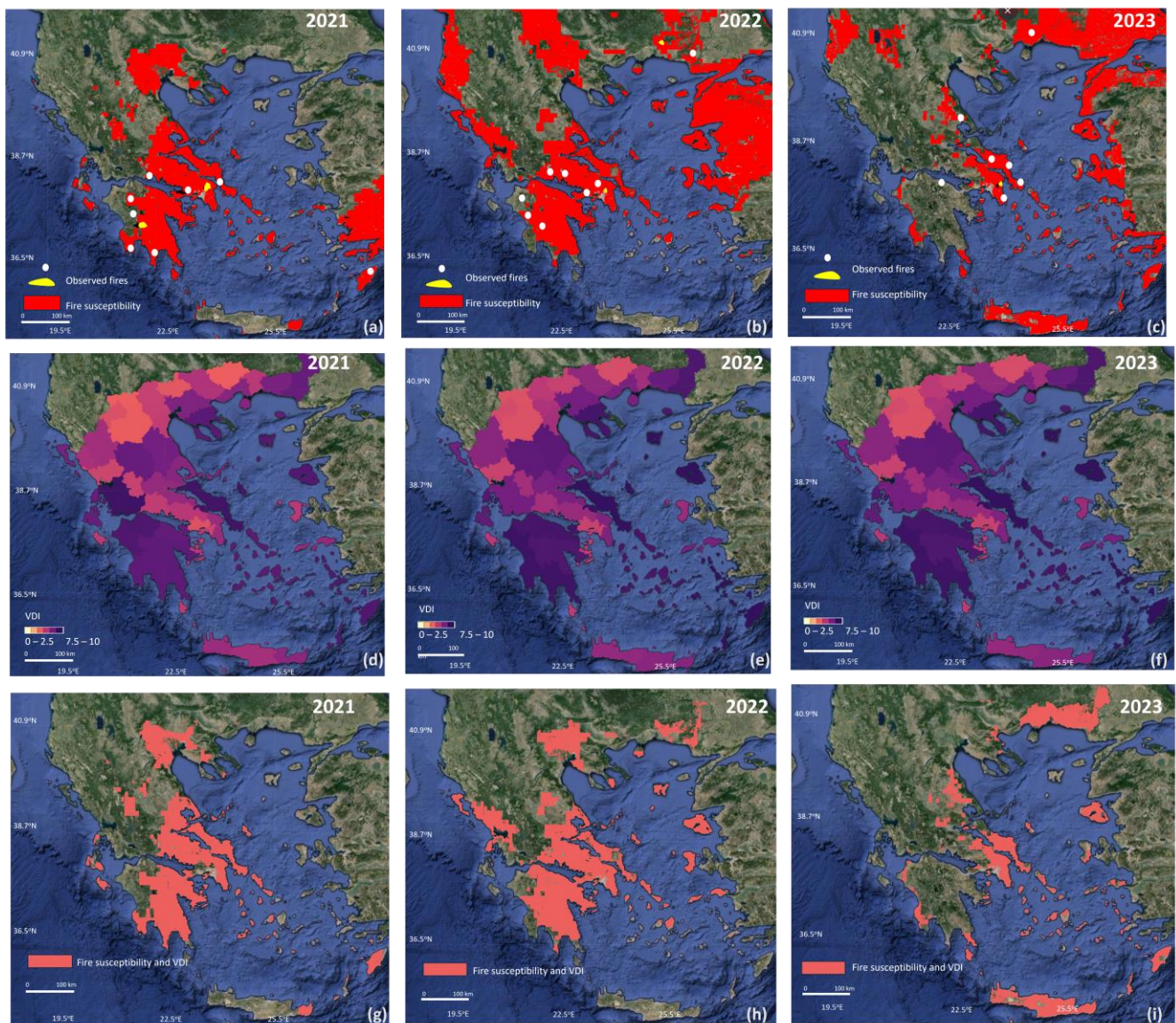

Figure 7. Spatial distribution of fire susceptibility (**a**–**c**), VDI at the NUTS3 level (**d**–**f**), and cross-tabulation results with fire susceptibility mapping of the present work (**g**–**i**) for Greece during 2021, 2022, and 2023.

Table 2. Results of the fire susceptibility assessment.

Year	Area (km²) with 0.13 < NDVI < 0.35	Area (km²) SM Anomaly < −5%	Fire-Susceptible Areas (km²)	Fire-Susceptible Areas in High-VDI Zones (km²)	Mean SM Anomaly (%)	Fire-Affected Areas within Fire-Susceptible Areas (km²)	Actual Affected Areas (km²)	Success Rate (%)
2023	116,503	22,536	20,132	19,355	−8.9	1485	1747	85
2022	157,231	26,709	23,531	22,187	−6.4	187	224	83
2021	161,732	28,311	22,587	22,534	−5.8	1132	1307	87

The examination of the fire susceptibility mapping, along with the VDI, aims to highlight areas susceptible to fire for a specified year, which at the same time, demonstrate medium to high vulnerability to disasters (VDI > 5) and associated increased social impact. Results of examination can be found in Figure 7.

4. Discussion

The results presented in Figure 6 indicate that the fire susceptibility is mostly controlled by the negative SM anomalies since the estimated NDVI range covers a substantial part of the country. This is mainly because of the prolonged drought period that resulted in vegetation stress conditions and decreased NDVI across the country. In their work, Moreno et al. [4] reported that MODIS NDVI values between 0.2 and 0.4 were observed during summer and autumn, which were found to be indicative of low humidity and increased flammability. However, the present work's results may differ because of the different time periods examined and the different study areas, as well as because of the different spatial resolutions of the examined NDVI products since the present work used Landsat 8 NDVI at 30 m, whereas Moreno et al. used [4] MODIS NDVI, which has a 500 m resolution.

SM results highlight the eastern mainland and the Aegean islands. A very characteristic case refers to the SM results, which clearly point out the high vulnerability of NE Greece during 2023 (Figure 6f) when the disastrous Alexandroupolis-Dadia wildfire occurred. It is worth mentioning that wildfires have long been affecting areas occupied by pine forests. These are typical of the Mediterranean landscape, especially in the central and southern parts of the country and the Aegean islands. Recently, however, areas like the Rhodope Mountain chain in the northeastern part of the country, occupied mainly by mixed forests (Oaks, plane trees, chestnuts, birch trees), were not considered fire-prone forest types. Still, they have been affected by large wildfire events twice during the study period (cases 3 and 6 in Table 1). Furthermore, the Papikio Mt. wildfire (case 6 in Table 1) lasted from late October to mid-November 2022, far outside the usual fire season. Traditionally, those rural areas were managed by local populations that removed dead excess vegetation from forest and pasture areas. Nowadays, depopulation has had a substantial impact on such traditional rural practices. This has also been observed in other Mediterranean countries [4]. In combination with the expected climate change impacts, the pattern of wildfire occurrence is changing, affecting northern areas [45] but also increasing the wildfire's destructive power. It is evident thus that the prolonged drought has impacted the usual temporal and spatial patterns of wildfires in Greece, which is an alarming and challenging issue for fire services in the country. Results presented herein converge to those indicated in previous works on the changing pattern of wildfire occurrence [4,45,46].

The susceptibility maps produced in this work successfully depicted all six wildfires used for validation (Figure 7a–c). Moreover, they identified the majority of wildfires comprised of the MODIS FIRMS product [37], with a success rate of 83% to 87%. Thus, the approach presented herein seems to provide a reliable approach for wildfire susceptibility mapping. It is also a tool of operational value since the SM and NDVI retrievals during spring may well help in defining areas where protective measures should be adopted to minimize fire risk, especially during the summer and autumn months. Since the latency of both examined remotely sensed products is within a week, it is clear that our approach can contribute to fire anticipation within realistic time frames.

Recent susceptibility mapping works have focused on average meteorological conditions (mean annual precipitation, mean annual temperature, wind speed) and various land variables like elevation, slope, and land cover type. They also evaluated several regression or machine learning methods to identify which performed best [19,21–23,47]. None of these works, however, evaluated soil moisture as a predicting parameter, whose value in fire modeling and fire susceptibility assessment had been highlighted in the U.S. and Australia in previous works [30,31]. In our work, it was shown that soil moisture is suitable for highlighting fire-susceptible areas also in the Mediterranean areas and can provide a near-real-time fire susceptibility approach. Moreover, it requires only minimum input data since it is based on remotely sensed soil moisture and NDVI. This is because soil moisture can be considered as a proxy for temperature, precipitation and humidity conditions, as it is closely related to those variables [48,49], and it is suitable for describing drought conditions. NDVI, on the other hand, can describe fuel availability, but it fails to respond in certain conditions, such as rapid drying [31]. Along with soil moisture, NDVI can be effective for fire susceptibility mapping. Previous works that quantified fire danger in terms of FWI were based on the availability of either weather data from meteorological stations [10] or modeled climate data [11], and the FWI has to be evaluated for the whole fire season. Our work can contribute to medium-term susceptibility mapping since it is based on SM and NDVI information from the preceding spring. Thus, it offers the advantage to public services of taking proactive measures earlier, whereas FWI is better suited for short-term fire danger assessments.

The examination of fire susceptibility mapping of the present work, alongside the EU VDI, highlighted areas where fire occurrence could potentially result in increased social impact. To the best of our knowledge, this is the first time that a fire susceptibility mapping has also incorporated the social dimension of fire disasters as included in the EU VDI. Thus, by comparing Figures 6 and 7, along with Table 2, it can be seen that all examined fires are within those high-impact zones and that the majority of fire-susceptible areas fall within the high-vulnerability areas of VDI.

An especially characteristic case is that of 2023, where the dramatic social impacts from the Rhodes Island wildfire and the Alexandroupolis-Dadia mega fire events are also reflected in Figure 7, as both those affected areas fall within high VDI regions. Thus, the combination of those two datasets successfully depicts areas where potential disasters may impose serious implications and should be the focus of protective fire management practices.

A limitation of the methodology is the spatial resolution of SM, which is too coarse for a fine delineation of fire-susceptible areas. However, downscaling approaches provide SMAP SM estimates at much higher spatial resolution, <1 km, which are found to be quite robust for drought monitoring [41,50–52]. Therefore, future efforts should focus on refining the spatial resolution of the fire susceptibility mapping. Additionally, since NDVI acquisitions are restricted by cloud cover conditions, extended cloud cover during springtime may result in considerable loss of data. However, this is not the case for SMAP SM retrievals, which are not impacted by cloud cover.

The approach presented herein may prove useful at the operational level. The forest fire risk maps issued daily during the fire season by the Greek General Secretariat for Civil Protection currently do not take into account soil moisture. Incorporating such an approach in the assessment of the fire risk maps can improve our knowledge of the areas where persisting drought conditions result in a high potential for a destructive fire. Thus, the fire susceptibility mapping presented in this work can contribute to the medium-term fire susceptibility assessment, while future research should focus on the incorporation of the soil moisture conditions in the daily fire risk maps to provide the short-term fire risk at the country level. The high fire potential of the areas where the two destructive wildfires in Rhodes and Alexandroupolis-Dadia happened could have been known two to three months before the events if drought conditions had been monitored with this approach and the highlighted areas had been integrated into the fire risk maps. Thus, firefighting authorities may prioritize actions in tackling wildfires, where areas with higher risk can

receive priority in determining firefighting actions and resource allocation. In addition, communities can be effectively informed in advance of the fire potential in their area, giving them enough time to take the necessary protective and preparatory measures. Finally, an analysis of the results of our fire susceptibility approach can help identify areas where the greatest social impacts are expected or where protected natural and cultural heritage areas and ecosystems have a high potential for fire.

5. Conclusions

In this work, a fire susceptibility mapping approach was presented, taking advantage of the SMAP L4 surface SM dataset. Initially, the predictive ability of SM regarding wildfire occurrence was examined and found to be significant. SMAP L4 and Landsat 8 NDVI time series were then analyzed for specific fire events in Greece for 2021, 2022, and 2023, and distinctive precursory patterns were identified and implemented into the fire susceptibility mapping approach. Results indicate that the proposed fire susceptibility method has a substantial predictive capability. The social impacts aspect was highlighted through the examination of the fire susceptibility mapping results alongside the EU Vulnerability to Disasters Index for Greece, depicting areas highly susceptible to fire occurrence and increased expected social impact.

References

1. Flannigan, M.D.; Krawchuk, M.A.; de Groot, W.J.; Wotton, B.M.; Gowman, L.M. Implications of Changing Climate for Global Wildland Fire. *Int. J. Wildland Fire* **2009**, *18*, 483–507. [CrossRef]
2. McLauchlan, K.K.; Higuera, P.E.; Miesel, J.; Rogers, B.M.; Schweitzer, J.; Shuman, J.K.; Tepley, A.J.; Varner, J.M.; Veblen, T.T.; Adalsteinsson, S.A.; et al. Fire as a Fundamental Ecological Process: Research Advances and Frontiers. *J. Ecol.* **2020**, *108*, 2047–2069. [CrossRef]
3. Xing, H.; Fang, K.; Yao, Q.; Zhou, F.; Ou, T.; Liu, J.; Zhou, S.; Jiang, S.; Chen, Y.; Bai, M.; et al. Impacts of Changes in Climate Extremes on Wildfire Occurrences in China. *Ecol. Indic.* **2023**, *157*, 111288. [CrossRef]
4. Moreno, M.; Bertolín, C.; Arlanzón, D.; Ortiz, P.; Ortiz, R. Climate Change, Large Fires, and Cultural Landscapes in the Mediterranean Basin: An Analysis in Southern Spain. *Heliyon* **2023**, *9*, e16941. [CrossRef] [PubMed]
5. Benscoter, B.; Thompson, D.; Waddington, J.; Flannigan, M.; Wotton, M.; Groot, W.; Turetsky, M. Interactive Effects of Vegetation, Soil Moisture and Bulk Density on Depth of Burning of Thick Organic Soils. *Int. J. Wildland Fire* **2011**, *20*, 418–429. [CrossRef]
6. Huang, Z.; Cao, C.; Chen, W.; Xu, M.; Dang, Y.; Singh, R.P.; Bashir, B.; Xie, B.; Lin, X. Remote Sensing Monitoring of Vegetation Dynamic Changes after Fire in the Greater Hinggan Mountain Area: The Algorithm and Application for Eliminating Phenological Impacts. *Remote Sens.* **2020**, *12*, 156. [CrossRef]
7. Gemitzi, A.; Koutsias, N. Assessment of Properties of Vegetation Phenology in Fire-Affected Areas from 2000 to 2015 in the Peloponnese, Greece. *Remote Sens. Appl.* **2021**, *23*, 100535. [CrossRef]
8. Sungmin, O.; Hou, X.; Orth, R. Observational Evidence of Wildfire-Promoting Soil Moisture Anomalies. *Sci. Rep.* **2020**, *10*, 11008.
9. Koutsias, N.; Allgöwer, B.; Kalabokidis, K.; Mallinis, G.; Balatsos, P.; Goldammer, J.G. Fire Occurrence Zoning from Local to Global Scale in the European Mediterranean Basin: Implications for Multi-Scale Fire Management and Policy. *IForest* **2016**, *9*, 195–204. [CrossRef]
10. Good, P.; Moriondo, M.; Giannakopoulos, C.; Bindi, M. The Meteorological Conditions Associated with Extreme Fire Risk in Italy and Greece: Relevance to Climate Model Studies. *Int. J. Wildland Fire* **2008**, *17*, 155. [CrossRef]
11. Papagiannaki, K.; Giannaros, T.M.; Lykoudis, S.; Kotroni, V.; Lagouvardos, K. Weather-Related Thresholds for Wildfire Danger in a Mediterranean Region: The Case of Greece. *Agric. For. Meteorol.* **2020**, *291*, 108076. [CrossRef]
12. Harris, S.; Nicholls, N.; Tapper, N. Forecasting Fire Activity in Victoria, Australia, Using Antecedent Climate Variables and ENSO Indices. *Int. J. Wildland Fire* **2014**, *23*, 173–184. [CrossRef]
13. Thomas Ambadan, J.; Oja, M.; Gedalof, Z.; Berg, A.A. Satellite-Observed Soil Moisture as an Indicator of Wildfire Risk. *Remote Sens.* **2020**, *12*, 1543. [CrossRef]
14. Gemitzi, A.; Koutsias, N. A Google Earth Engine Code to Estimate Properties of Vegetation Phenology in Fire Affected Areas—A Case Study in North Evia Wildfire Event on August 2021. *Remote Sens. Appl.* **2022**, *26*, 100720. [CrossRef]
15. Alcasena, F.J.; Ager, A.A.; Salis, M.; Day, M.A.; Vega-Garcia, C. Optimizing Prescribed Fire Allocation for Managing Fire Risk in Central Catalonia. *Sci. Total Environ.* **2018**, *621*, 872–885. [CrossRef] [PubMed]
16. Aparício, B.A.; Pereira, J.M.C.; Santos, F.C.; Bruni, C.; Sá, A.C.L. Combining Wildfire Behaviour Simulations and Network Analysis to Support Wildfire Management: A Mediterranean Landscape Case Study. *Ecol Indic* **2022**, *137*, 108726. [CrossRef]
17. Fares, S.; Bajocco, S.; Salvati, L.; Camarretta, N.; Dupuy, J.L.; Xanthopoulos, G.; Guijarro, M.; Madrigal, J.; Hernando, C.; Corona, P. Characterizing Potential Wildland Fire Fuel in Live Vegetation in the Mediterranean Region. *Ann. For. Sci.* **2017**, *74*, 1. [CrossRef]
18. Ba, R.; Song, W.; Lovallo, M.; Zhang, H.; Telesca, L. Informational Analysis of MODIS NDVI and EVI Time Series of Sites Affected and Unaffected by Wildfires. *Phys. A Stat. Mech. Its Appl.* **2022**, *604*, 127911. [CrossRef]
19. Akıncı, H.A.; Akıncı, H. Machine Learning Based Forest Fire Susceptibility Assessment of Manavgat District (Antalya), Turkey. *Earth Sci. Inform.* **2023**, *16*, 397–414. [CrossRef]
20. Zhang, G.; Wang, M.; Liu, K. Forest Fire Susceptibility Modeling Using a Convolutional Neural Network for Yunnan Province of China. *Int. J. Disaster Risk Sci.* **2019**, *10*, 386–403. [CrossRef]
21. Das, J.; Mahato, S.; Joshi, P.K.; Liou, Y.-A. Forest Fire Susceptibility Zonation in Eastern India Using Statistical and Weighted Modelling Approaches. *Remote Sens.* **2023**, *15*, 1340. [CrossRef]
22. Pragya; Kumar, M.; Tiwari, A.; Majid, S.I.; Bhadwal, S.; Sahu, N.; Verma, N.K.; Tripathi, D.K.; Avtar, R. Integrated Spatial Analysis of Forest Fire Susceptibility in the Indian Western Himalayas (IWH) Using Remote Sensing and GIS-Based Fuzzy AHP Approach. *Remote Sens.* **2023**, *15*, 4701. [CrossRef]
23. Achu, A.L.; Thomas, J.; Aju, C.D.; Gopinath, G.; Kumar, S.; Reghunath, R. Machine-Learning Modelling of Fire Susceptibility in a Forest-Agriculture Mosaic Landscape of Southern India. *Ecol. Inform.* **2021**, *64*, 101348. [CrossRef]
24. Jensen, D.; Reager, J.T.; Zajic, B.; Rousseau, N.; Rodell, M.; Hinkley, E. The Sensitivity of US Wildfire Occurrence to Pre-Season Soil Moisture Conditions across Ecosystems. *Environ. Res. Lett.* **2018**, *13*, 014021. [CrossRef]
25. Walters, A.; Fang, B.; Lakshmi, V. Using Earth Observations to Measure Hydrological Conditions Before, During, and After Wildfires in the Feather River Watershed. *IEEE J. Sel. Top. Appl. Earth Obs. Remote Sens.* **2024**, *17*, 6972–6985. [CrossRef]
26. Westerling, A.L.; Hidalgo, H.G.; Cayan, D.R.; Swetnam, T.W. Warming and Earlier Spring Increase Western U.S. Forest Wildfire Activity. *Science* **2006**, *313*, 940–943. [CrossRef]
27. Wang, L.; Quan, X.; He, B.; Yebra, M.; Xing, M.; Liu, X. Assessment of the Dual Polarimetric Sentinel-1A Data for Forest Fuel Moisture Content Estimation. *Remote Sens.* **2019**, *11*, 1568. [CrossRef]

28. Jia, S.; Kim, S.H.; Nghiem, S.V.; Kafatos, M. Estimating Live Fuel Moisture Using SMAP L-Band Radiometer Soil Moisture for Southern California, USA. *Remote Sens.* **2019**, *11*, 1575. [CrossRef]

29. Sharma, S.; Dhakal, K. Boots on the Ground and Eyes in the Sky: A Perspective on Estimating Fire Danger from Soil Moisture Content. *Fire* **2021**, *4*, 45. [CrossRef]

30. Sazib, N.; Bolten, J.D.; Mladenova, I.E. Leveraging NASA Soil Moisture Active Passive for Assessing Fire Susceptibility and Potential Impacts Over Australia and California. *IEEE J. Sel. Top. Appl. Earth Obs. Remote Sens.* **2022**, *15*, 779–787. [CrossRef]

31. Sharma, S.; Carlson, J.D.; Krueger, E.S.; Engle, D.M.; Twidwell, D.; Fuhlendorf, S.D.; Patrignani, A.; Feng, L.; Ochsner, T.E. Soil Moisture as an Indicator of Growing-Season Herbaceous Fuel Moisture and Curing Rate in Grasslands. *Int. J. Wildland Fire* **2021**, *30*, 57. [CrossRef]

32. Mladenova, I.E.; Bolten, J.D.; Crow, W.T.; Sazib, N.; Cosh, M.H.; Tucker, C.J.; Reynolds, C. Evaluating the Operational Application of SMAP for Global Agricultural Drought Monitoring. *IEEE J. Sel. Top. Appl. Earth Obs. Remote Sens.* **2019**, *12*, 3387–3397. [CrossRef]

33. Sibilia, G.; Salvi, A.; Antofie, A.; Rodomonti, T.-E.; Marzi, K.; Gyenes, S. *Towards a European Wide Vulnerability Framework A Flexible Approach for Vulnerability Assessment Using Composite Indicators*; European Union: Brussels, Belgium, 2022.

34. Eklund, L.; Sibilia, A.; Salvi, A.; Antofie, T.; Rodomonti, D.; Salari, S.; Poljansek, K.; Marzi, S.; Gyenes, Z.; Corban, C. *Towards a European Wide Vulnerability Framework*; European Union: Brussels, Belgium, 2023. [CrossRef]

35. Hellenic Fire Service Hellenic Fire Service. Available online: https://www.fireservice.gr/el (accessed on 1 February 2023).

36. Copernicus European Forest Fire Information System (EFFIS). Available online: https://effis.jrc.ec.europa.eu/ (accessed on 2 March 2024).

37. NASA MODIS Collection 6 NRT Hotspot/Active Fire Detections MCD14DL. Available online: https://earthdata.nasa.gov/firms (accessed on 19 April 2024).

38. Bechtold, M.; De Lannoy, G.; Koster, D.; Crow, W.T.; Kimball, J.S.; Liu, Q.; Bechtold, M. *SMAP L4 Global 3-Hourly 9 Km EASE-Grid Surface and Root Zone Soil Moisture Analysis Update, Version 7*; National Snow and Ice Data Center: Boulder, CO, USA, 2022.

39. Australian Goevernment, Department of Agriculture, Fisheries and Forestry. *National Soil Strategy*; Australian Goevernment, Department of Agriculture, Fisheries and Forestry: Canberra, Australia, 2021.

40. Reichle, R.H.; Liu, Q.; Koster, R.D.; Crow, W.T.; De Lannoy, G.J.M.; Kimball, J.S.; Ardizzone, J.V.; Bosch, D.; Colliander, A.; Cosh, M.; et al. Version 4 of the SMAP Level-4 Soil Moisture Algorithm and Data Product. *J. Adv. Model Earth Syst.* **2019**, *11*, 3106–3130. [CrossRef]

41. Dong, J.; Crow, W.; Reichle, R.; Liu, Q.; Lei, F.; Cosh, M.H. A Global Assessment of Added Value in the SMAP Level 4 Soil Moisture Product Relative to Its Baseline Land Surface Model. *Geophys. Res. Lett.* **2019**, *46*, 6604–6613. [CrossRef]

42. Gorelick, N.; Hancher, M.; Dixon, M.; Ilyushchenko, S.; Thau, D.; Moore, R. Google Earth Engine: Planetary-Scale Geospatial Analysis for Everyone. *Remote Sens. Environ.* **2017**, *202*, 18–27. [CrossRef]

43. Chan, S.K.; Bindlish, R.; O'Neill, P.E.; Njoku, E.; Jackson, T.; Colliander, A.; Chen, F.; Burgin, M.; Dunbar, S.; Piepmeier, J.; et al. Assessment of the SMAP Passive Soil Moisture Product. *IEEE Trans. Geosci. Remote Sens.* **2016**, *54*, 4994–5007. [CrossRef]

44. Colliander, A.; Jackson, T.J.; Bindlish, R.; Chan, S.; Das, N.; Kim, S.B.; Cosh, M.H.; Dunbar, R.S.; Dang, L.; Pashaian, L.; et al. Validation of SMAP Surface Soil Moisture Products with Core Validation Sites. *Remote Sens. Environ.* **2017**, *191*, 215–231. [CrossRef]

45. Adámek, M.; Jankovská, Z.; Hadincová, V.; Kula, E.; Wild, J. Drivers of Forest Fire Occurrence in the Cultural Landscape of Central Europe. *Landsc. Ecol.* **2018**, *33*, 2031–2045. [CrossRef]

46. Vilar, L.; Herrera, S.; Tafur-García, E.; Yebra, M.; Martínez-Vega, J.; Echavarría, P.; Martín, M.P. Modelling Wildfire Occurrence at Regional Scale from Land Use/Cover and Climate Change Scenarios. *Environ. Model. Softw.* **2021**, *145*, 105200. [CrossRef]

47. Pourghasemi, H.R.; Gayen, A.; Lasaponara, R.; Tiefenbacher, J.P. Application of Learning Vector Quantization and Different Machine Learning Techniques to Assessing Forest Fire Influence Factors and Spatial Modelling. *Environ. Res.* **2020**, *184*, 109321. [CrossRef]

48. Tang, C.; Chen, D. Interaction between Soil Moisture and Air Temperature in the Mississippi River Basin. *J. Water Resour. Prot.* **2017**, *9*, 1119–1131. [CrossRef] [PubMed]

49. Sehler, R.; Li, J.; Reager, J.; Ye, H. Investigating Relationship Between Soil Moisture and Precipitation Globally Using Remote Sensing Observations. *J. Contemp. Water Res. Educ.* **2019**, *168*, 106–118. [CrossRef]

50. Fang, B.; Lakshmi, V.; Bindlish, R.; Jackson, T. AMSR2 Soil Moisture Downscaling Using Temperature and Vegetation Data. *Remote Sens.* **2018**, *10*, 1575. [CrossRef]

51. Fang, B.; Kansara, P.; Dandridge, C.; Lakshmi, V. Drought Monitoring Using High Spatial Resolution Soil Moisture Data over Australia in 2015–2019. *J. Hydrol.* **2021**, *594*, 125960. [CrossRef]

52. Fang, B.; Lakshmi, V.; Cosh, M.; Liu, P.W.; Bindlish, R.; Jackson, T.J. A Global 1-Km Downscaled SMAP Soil Moisture Product Based on Thermal Inertia Theory. *Vadose Zone J.* **2022**, *21*, e20182. [CrossRef]